

Investigating the Design Space of Visual Grounding in Multimodal Large Language Model

Weitai Kang^{1,*}, Weiming Zhuang², Zhizhong Li², Yan Yan¹, Lingjuan Lyu^{2,†}
¹University of Illinois Chicago, ²Sony AI

Abstract

Fine-grained multimodal capability in Multimodal Large Language Models (MLLMs) has emerged as a critical research direction, particularly for tackling the visual grounding (VG) problem. Despite the strong performance achieved by existing approaches, they often employ disparate design choices when fine-tuning MLLMs for VG, lacking systematic verification to support these designs. To bridge this gap, this paper presents a comprehensive study of various design choices that impact the VG performance of MLLMs. We conduct our analysis using LLaVA-1.5, which has been widely adopted in prior empirical studies of MLLMs. While more recent models exist, we follow this convention to ensure our findings remain broadly applicable and extendable to other architectures. We cover two key aspects: (1) exploring different visual grounding paradigms in MLLMs, identifying the most effective design, and providing our insights; and (2) conducting ablation studies on the design of grounding data to optimize MLLMs’ fine-tuning for the VG task. Finally, our findings contribute to a stronger MLLM for VG, achieving improvements of +5.6% / +6.9% / +7.0% on RefCOCO+/+g over the LLaVA-1.5.

1. Introduction

Visual grounding (VG) is a crucial vision-language learning task that aims to predict the location of an object in an image based on a given sentence [11, 12, 14, 16, 28, 31, 51]. It facilitates fine-grained cooperation between humans and AI agents in real-world scenarios [10, 13, 20] and benefits multimodal reasoning systems, such as visual question answering [7, 35, 43] and image captioning [1, 3, 50]. Early methods develop specialist models [6, 12, 14, 47] with architectures tailored for visual grounding. Extending beyond task-specific solutions, later approaches introduce unified models [21, 26, 27, 41, 42, 44, 48, 54], which benefit VG learning through integrating knowledge

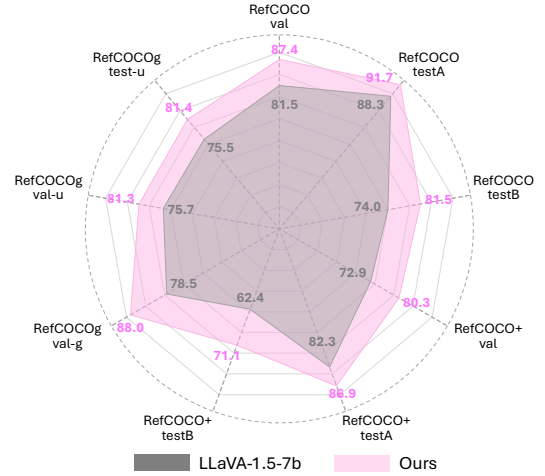


Figure 1. Using LLaVA-1.5-7B as the baseline, we conduct a comprehensive empirical study focusing on the design of visual grounding in Multimodal Large Language Models. We identify several improved designs while also ruling out certain potential alternatives. Finally, we integrate all the best designs, achieving a significant improvement over the baseline.

from multiple tasks. Recently, researchers explore incorporating VG capabilities into Multimodal Large Language Models (MLLMs) [2, 8, 24, 30, 45, 49, 56]. Unlike unified models that require extensive fine-grained labels across tasks, MLLMs inherit strong reasoning abilities from LLMs [5, 39, 40] and general visual understanding from vision foundation models [29, 32, 53], both of which were trained on large-scale unlabeled data. This enables MLLMs to not only achieve strong VG performance after fine-tuning but also support complex multimodal interactions, such as multi-turn reasoning, making them promising for VG.

The idea of incorporating VG capability into MLLMs is inspired by Pix2Seq [4], which pioneered the reformulation of bounding box regression as classification by discretizing values into different bins. Despite the rapid progress in adapting MLLMs for VG, current studies often present disparate design choices, lacking a comprehensive experimental justification. Meanwhile, existing empirical studies on the design of MLLMs [15, 19, 37] primarily focus on training recipes [15, 19], model structure choices [19, 37],

*Work done during internship at Sony AI

†Corresponding author

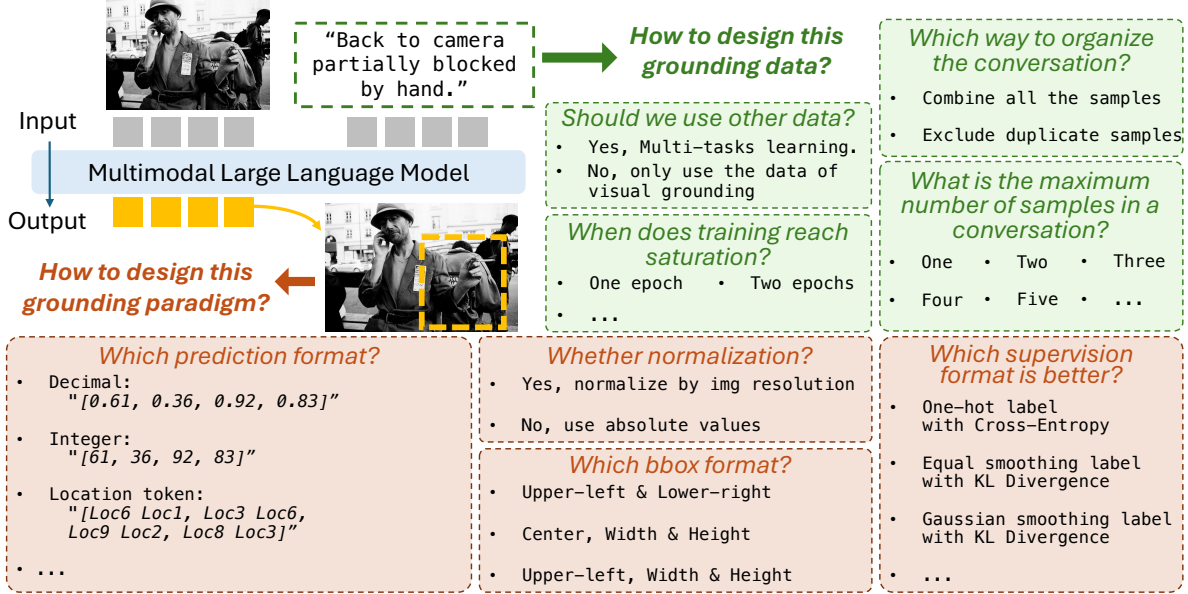


Figure 2. We conduct systematic ablation studies to explore different design choices for building visual grounding ability in Multimodal Large Language Model. We investigate two main aspects: **Grounding paradigm design** and **Grounding data design**.

and textual benchmarks [15, 19] such as visual question answering and image captioning. However, these efforts are insufficient to fully characterize MLLMs’ potential in fine-grained multimodal reasoning, as they have not thoroughly explored the highly diverse VG design in MLLMs, which is a crucial part of MLLMs to serve as generalist models. Moreover, within the VG community, advancing MLLMs to excel in this domain [2, 8, 30, 45, 49] remains a topic requiring further exploration.

To address these gaps, we systematically investigate different design choices for building VG ability in MLLMs, which complements previous studies. Following the convention of prior empirical studies on MLLMs [15, 37], we ground our research by using LLaVA-1.5 [24], one of the most popular works in MLLM development, as the baseline. As shown in Fig. 2, we systematically study on the design choices in the grounding paradigm design and the grounding data design for VG in MLLMs.

Specifically, we highlight four key contributions. First, for grounding paradigm design, **we systematically examine how bounding boxes (bbox) should be represented**, e.g., whether normalization is necessary. Notably, our exploration extends beyond existing MLLM designs (e.g., different bbox prediction formats) to incorporate new alternative approaches inspired from non-MLLM domains (e.g., different bbox supervision formats). Second, for grounding data design, **we identify the effective data configurations**, and reveal that using pure VG data and deduplicated conversational samples leads to improved learning efficiency. Third, **we provide insights into those better design choices**. We introduce a similarity-based correla-

tion metric to quantify the enhancements on the spatial semantics of coordinate tokens brought by training with the one-hot label and cross-entropy loss. This metric could be a useful tool for analyzing MLLM’s VG behavior in future research. Finally, by incorporating the optimal design choices identified in our findings, **we achieve substantial improvements over the baseline, LLaVA-1.5**, as shown in Fig. 1. Crucially, we not only reveal the effective designs in MLLMs—encompassing both existing and unexplored approaches—but also uncover the ineffective designs, despite their prior adoption and perceived potential. Our findings offer clear guidelines for the future development of MLLM-based VG.

2. Background

2.1. Related Work

Classification Paradigm in Fine-Grained Task. Many works adopt the classification paradigm for fine-grained visual recognition, including those in object detection, visual grounding, and human pose estimation. Pix2seq [4], OFA [41], and KOSMOS-2 [30] discretize image locations and introduce extra vocabularies into language modeling to represent bounding box coordinates. Methods such as Shikra [2], LLaVA-1.5 [24], and Pink [45] directly treat the textual representation of bounding boxes as prediction targets and classify each digit in those decimal values using language modeling. Each training sample is organized as a conversation, transforming the visual grounding problem into a question-answering format. Ferret [49], Ferret-v2 [56], and MM1.5 [55] convert decimals into integers by

quantizing each coordinate into one of 1000 discrete bins and classifying the textual representation of these integer values using language modeling. The values are not normalized by image resolution. In human pose estimation, SimCC [22] discretizes each keypoint location into discrete bins and classifies the bins. It introduces label smoothing to account for the spatial relevance of adjacent bins. In addition to explicitly generating bounding box coordinates, some MLLMs employ an implicit representation for referring image segmentation [18, 33, 34]. For example, Lisa [18] uses a special language token to indicate an object and decodes the segmentation mask from the hidden state of this token. Yet, due to differences in model structure, task, data, and training recipe, the optimal design for visual grounding in MLLMs remains an open question.

Empirical Study of MLLMs. As MLLMs continue to advance the field of vision-language learning, researchers have begun to explore their design space by empirical studies. Prismatic [15] investigates the training recipe of MLLMs based on LLaVA-1.5 [24]. Eagle [37] explores the design space for MLLMs, focusing on vision encoders and input resolutions via question-answering benchmarks. Idefics2 [19] conducts extensive experiments on pretrained models, architectures, data, and training methods, benchmarking them on question-answering and captioning tasks. However, none of these works provide empirical studies on the design choices for visual grounding in MLLMs.

2.2. Preliminaries

Model Architecture. For an input image, we use a pre-trained CLIP-ViT-L-336px [32] as the visual encoder. Its output visual features are projected into the LLM’s word embedding space via a two-layer MLP (vision-language connector), producing a sequence of visual tokens. The corresponding texts for questions and answers are tokenized and projected into text tokens. The visual tokens and text tokens are then concatenated into a single sequence. Given the initial part of the sequence, the LLM, Vicuna-7B-v1.5 [5], predicts the next token based on the preceding tokens. Unless specified otherwise, we use the cross-entropy loss. Only the tokens corresponding to the answer text are considered as the supervised learning targets.

Implementation. We use the official codebase from LLaVA-1.5 [23] and retain its training hyperparameters to ensure reproducibility. We adopt the pretrained vision-language connector from LLaVA-1.5 and fine-tune both the connector and the LLM. We extract visual grounding data from LLaVA-1.5’s 665K multimodal instruction-tuning examples to conduct systematic ablation studies. In total, we extract 112,370 visual grounding conversational

samples originating from RefCOCO+/g [16, 28] and Visual Genome [17], with additional annotations provided by the LLaVA-1.5 authors. Each sample consists of an image and multiple rounds of question-answering for the visual grounding task. The remaining samples, including visual question-answering data from Hudson and Manning [9], Liu et al. [25], Sidorov et al. [38] and language-only question-answering data from ShareGPT [36], are used in studying the synergistic effect of multitask learning in Sec. 4.1. Without specified otherwise, we use only visual grounding data for training by default.

Evaluation Suite. We follow common practices [6, 10–12, 14, 46, 47, 52] to evaluate visual grounding performance on RefCOCO+/g [16, 28]. RefCOCO emphasizes brief descriptions with spatial references, RefCOCO+ focuses solely on appearance-based descriptions, and RefCOCOg centers on extended, detailed descriptions. We evaluate bounding box prediction accuracy, considering a predicted bounding box correct if its Intersection over Union (IoU) with the ground-truth bounding box exceeds 0.5.

We emphasize that this is an empirical study aimed at laying the foundation for the future development of visual grounding in MLLMs. *To ensure the fairness of our ablation studies and the rigor of our findings, we intentionally refrain from comparing with other MLLMs, as disparities in data utilization, training scope, and model parameters would provide limited meaningful insights in our systematic experiments.*

3. Grounding Paradigm Design

In this section, we investigate the grounding paradigm designs of MLLMs, including the prediction format in Sec. 3.1, the normalization type in Sec. 3.2, the supervision format in Sec. 3.3, and the bounding box format in Sec. 3.4.

3.1. Prediction Format

Following the classification paradigms outlined in Sec. 2.1, we examine five candidate formats for bounding box targets, covering both explicit representations in various formats [4, 24, 30, 49] and implicit approaches [8, 18, 34].

1) *Decimal format.* Following Chen et al. [2], Liu et al. [24], Xuan et al. [45], the bbox values range from 0 to 1 after normalization by the image resolution. For instance, the MLLM may be trained to predict the string “[0.17, 0.23, 0.8, 0.65]”.

2) *Integer format.* Following approaches in [49, 55, 56], we convert the decimals to integers by multiplying them by 100, yielding integer strings such as “[17, 23, 80, 65]”. The conversion is performed on normalized ranges, which ensures consistency with other formats in our comparison. However, note that the aforementioned methods adopt the

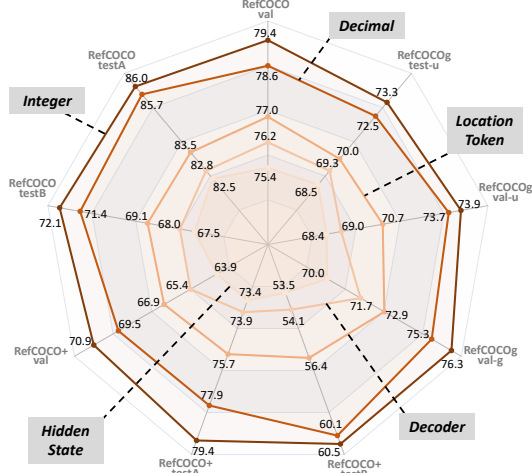


Figure 3. We explore the choices on the prediction format for MLLM’s visual grounding paradigm design. We find that explicit prediction formats, like *decimal*, *integer*, and *location token* formats universally outperform implicit prediction formats (*hidden state*, *decoder*). And *integer* format provides the best performance.

absolute values without normalization by the image resolution. We will discuss the normalization design in Sec. 3.2.

3) *Location token format*. To explore the use of new vocabularies to represent location, as in Chen et al. [4], Peng et al. [30], Wang et al. [41], we discretize the image coordinates into n bins. We then add extra vocabulary tokens to represent these bins. In alignment with the original vocabulary, which only has ten words from 0 to 9 to represent digits, we add ten new location words, from “*Loc0*” to “*Loc9*”. For instance, the MLLM predicts two tokens, “*Loc1 Loc7*”, to indicate the 17th bin. We set n to 101 to match the numerical precision of the previous format.

4) *Hidden state format*. Inspired by Lisa [18], PixelLM [34], and AnyRef [8], we introduce a special token, “*<Det>*”, to the vocabulary. The model needs to predict this token in language modeling and decode its hidden state to predict the bounding box using traditional object detection losses. To evaluate the effectiveness of this format in a simplified setting, we use a three-layer MLP to decode the hidden state.

5) *Decoder format*. To further investigate the ideas from Lisa, PixelLM, and AnyRef while preserving approximately equivalent model parameters for a fair comparison, we augment the *hidden state* format by adding three extra transformer layers as a decoder. This allows the hidden state to perform cross-attention on the vision features extracted by the vision encoder before predicting the bounding box.

Results. Under the experimental setup outlined in Sec. 2.2, where models are trained for one epoch on visual grounding data, we observe two key findings, as illustrated in Fig. 3: 1) Within a comparable model parameter scope, explicit prediction formats—namely *decimal*, *integer*, and *lo-*

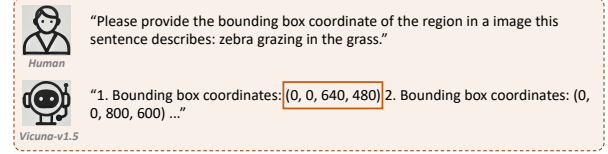


Figure 4. To investigate why the *integer* format is superior in MLLM’s visual grounding paradigm, we examine the behavior of the pretrained LLM model, Vicuna-v1.5 [5], from which our MLLM is fine-tuned. We find that the pretrained LLM inherently utilizes the *integer* format, making it more natural and effective to continue using this format during fine-tuning.

cation token formats—are more effective for training than implicit formats, such as *hidden state* and *decoder* formats. 2) Among the explicit formats, the *integer* format achieves the best performance, significantly surpassing the *location token* format and slightly outperforming the *decimal* format.

Discussion. To understand why the *integer* format outperforms others in MLLM’s visual grounding paradigm, we examine the behavior of the pretrained LLM model, Vicuna-v1.5, from which our MLLM is fine-tuned. As shown in Fig. 4, when we prompt Vicuna-v1.5 with a visual grounding task using only the description (without an image), we find that the pretrained LLM inherently adopts the *integer* format. This suggests that using the *integer* during fine-tuning may better align with the model’s pretrained knowledge, making the training more effective.

3.2. Normalization Type

Given the varying choices in previous works [2, 24, 49, 55, 56] on whether the bounding box should be normalized by image resolution, we conduct a comprehensive comparison by evaluating each normalization type—*normalized* or *unnormalized*—across three prediction formats: *decimal*, *integer*, and *decoder*.

1) *Normalized type*. Following Chen et al. [2] and Liu et al. [24], the bounding box is normalized by the image resolution. This setting is adopted in many existing visual grounding methods [6, 11, 12, 14]. For example, given a 640×640 image and a bounding box of “[32, 32, 320, 320]”, the *normalized* type in *decimal* format is “[0.05, 0.05, 0.5, 0.5]”, and in *integer* format, it is “[5, 5, 50, 50]”.

2) *Unnormalized type*. In contrast, You et al. [49], Zhang et al. [55, 56] adopt an *unnormalized* type, where the bounding box retains its absolute values without normalization. In this case, for the same example, its *decimal* format is obtained by dividing by a fixed maximum value (e.g., 1280), resulting in “[0.025, 0.025, 0.25, 0.25]”, while its *integer* format remains as the absolute values: “[32, 32, 320, 320]”.

Results. As shown in Fig. 5(a,b,c), under a fair experimental setting and comprehensive evaluation, we find that the more common choice, *normalized type*, consistently outperforms the *unnormalized type*.

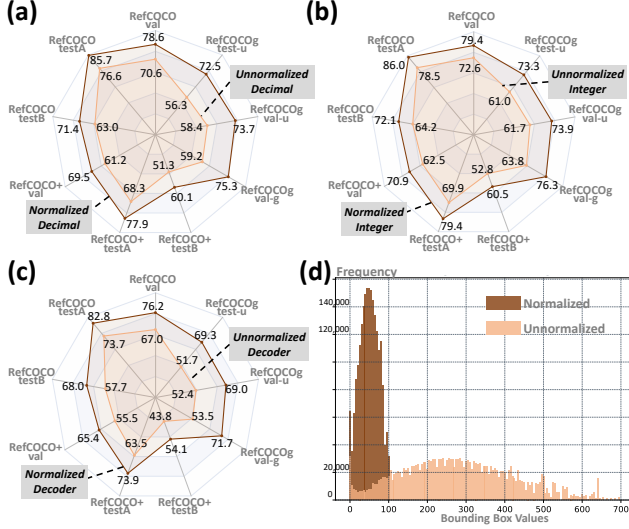


Figure 5. (a,b,c): Performance comparison of normalization types – *normalized* and *unnormalized* types under three prediction formats – *decimal*, *integer*, and *decoder* formats. (d): Frequency comparison of *normalized* and *unnormalized* types. The bar chart shows the frequency of unique location values, illustrating the concentrated distribution of *normalized* types and the long-tailed distribution of *unnormalized* types.

Discussion. Using the *integer* format, we analyze the frequency distribution of location values in the training dataset. As shown in the histogram in Fig. 5(d), the distribution for the *normalized* type is notably more concentrated, as normalization enables a coordinate token to represent various absolute location values across different image resolutions. In contrast, the *unnormalized* type exhibits a broader range of location values, leading to increased variability and less efficient training compared to the *normalized* type.

To quantitatively evaluate the long-tailed distribution, we compute Excess Kurtosis (EK), which measures the sharpness and tail heaviness of a distribution. A higher EK (positive value) indicates heavier tails and a stronger long-tail effect, while a lower EK (negative value) suggests lighter tails and fewer extreme values. For the *normalized* type, the EK is -0.7595 , indicating relatively light tails. In contrast, the *unnormalized* type has a EK of 0.6611 , signifying a more pronounced long-tail effect. We further validate these observations using the *decimal* format, which yields consistent results: for the *normalized* type, EK is -0.7595 ; for the *unnormalized* type, EK is 0.6677 . In summary, the *normalized* type produces a more balanced distribution with lighter tails, which is advantageous for mitigating long-tail effects in training.

3.3. Supervision Format

MLLMs use cross-entropy loss with one-hot encoded label as supervision. In human pose estimation, SimCC [22], a method that also adopts the classification paradigm, incor-

Format	RefCOCO			RefCOCO+			RefCOCOg			Ave.↓
	val	testA	testB	val	testA	testB	val-g	val-u	test-u	Rank
<i>Using Decimal Prediction Format</i>										
<i>One-hot</i>	78.6	85.7	71.4	69.5	77.9	60.1	75.3	73.7	72.5	1.0
<i>Equal</i>	77.9	85.0	70.6	68.5	77.8	58.1	74.2	72.0	72.2	3.2
<i>Gaussian</i>	78.4	85.3	70.9	69.0	77.9	59.3	74.8	72.4	72.2	2.0
<i>Gaussian^W</i>	77.8	85.7	70.0	68.3	77.1	57.4	74.7	72.1	71.6	3.4
<i>Using Integer Prediction Format</i>										
<i>One-hot</i>	79.4	86.0	72.1	70.9	79.4	60.5	76.3	73.9	73.3	1.4
<i>Equal</i>	79.4	86.2	71.0	70.0	78.8	59.5	76.2	74.0	73.2	2.2
<i>Gaussian</i>	79.8	86.4	71.0	70.1	79.2	59.9	76.0	73.6	72.9	2.1
<i>Gaussian^W</i>	73.5	77.3	64.2	64.4	71.5	54.3	60.0	67.8	66.1	4.0

Table 1. Performance of different supervision formats across various benchmarks. *Gaussian^W* indicates *weighted Gaussian label smoothing*. The *one-hot* format consistently achieves the highest rank, followed by the *Gaussian label smoothing* format, in both *decimal* and *integer* prediction formats. The average rank is computed by averaging rankings across different benchmarks.

porates *label smoothing* to address annotation noise. Given its demonstrated effectiveness in the pixel-level task, we hypothesize that *label smoothing* might similarly enhance the performance of MLLM in visual grounding. Therefore, we investigate this potential for a thorough and comprehensive empirical study.

1) *One-hot*. MLLMs employ an autoregressive language modeling approach, wherein the ground-truth of each token is represented by the one-hot encoding and the objective is to minimize the cross-entropy loss.

2) *Equal label smoothing*. SimCC [22] adopts the equal label smoothing technique in keypoint location prediction. Specifically, the ground-truth label is represented as a probability distribution, where the correct category is assigned a high probability value (0.9), while the remaining categories receive a uniform low probability (0.1). This technique aims to mitigate noise introduced by human annotations. The corresponding loss function is the KL-Divergence loss.

3) *Gaussian label smoothing*. Instead of uniformly assigning low probabilities to all incorrect categories, SimCC [22] further introduces *Gaussian label smoothing*, where the ground-truth probability distribution follows a Gaussian distribution centered at the correct category. This approach ensures that locations closer to the ground truth receive higher probabilities, effectively capturing the varying loss intensity due to spatial proximity. We set the standard deviation to 0.5, as it yields the best performance.

4) *Weighted Gaussian label smoothing*. We further consider a crucial factor specific to visual grounding in MLLMs. When predicting a value autoregressively, errors in different digits of the value have varying impacts. For example, given a target value of “0.17,” an error of one unit in the tenths place results in an overall error of “0.1,” whereas the same error in the hundredths place leads to only “0.01.”

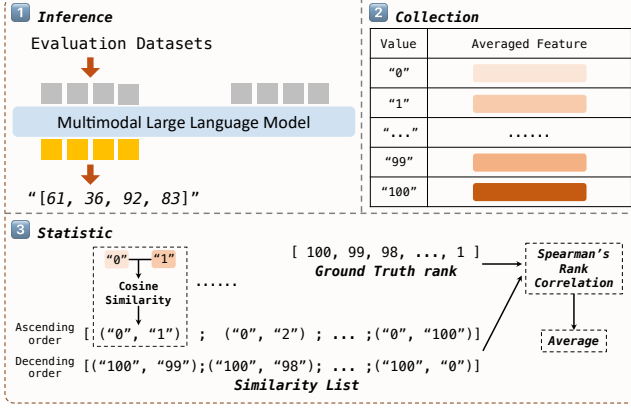


Figure 6. Illustration of the similarity-based correlation metric. After collecting the feature of different coordinate values, we compute token similarities by selecting 0 and 100 as anchor points and measuring cosine similarity between coordinates and anchors in ascending and descending order, respectively. We then use Spearman’s Rank Correlation (ρ) to evaluate the alignment between the two similarity lists and the ground-truth rank list. Finally, we average the two ρ results from both lists.

To account for this, we assign lower variance to higher-magnitude digits. Specifically, for the *decimal* format, we set the standard deviations for the ones, tenths, and hundredths places to 0.1, 0.5, and 0.7, respectively. For the *integer* format, we set the standard deviations for the tens and ones places to 0.1 and 0.5, respectively.

Results. As shown in Tab. 1, the most commonly used *one-hot* supervision format outperforms others across most benchmarks, regardless of whether the prediction format is *decimal* or *integer*. To quantify the relative effectiveness of different supervision formats, we rank them across multiple benchmarks and compute their average rank. The *one-hot* format achieves the highest rank, followed by the *Gaussian label smoothing* format.

Discussion. To investigate whether coordinate tokens trained with the *one-hot* format encode spatial semantics, we propose a similarity-based correlation metric. Our hypothesis is that coordinates closer in value should exhibit more similar token representations. As illustrated in Fig. 6, we follow a three-step process: 1) We run inference on all evaluation datasets. 2) For each coordinate in the model’s output, we extract its corresponding token features from the last layer and compute their average. 3) We select 0 and 100 as anchor points and compute the cosine similarity between each coordinate and the anchor—one in ascending order and the other in descending order—thus generating two similarity lists. If our hypothesis holds perfectly, these lists should follow a strictly decreasing order. To quantitatively evaluate this hypothesis, we construct a ground-truth ranking list from 100 to 1 in descending order, corresponding to the expected behavior under a perfectly valid

Format	RefCOCO		RefCOCO+		RefCOCOg		Ave.↓	
	val	testA	testB	val	testA	testB	val-g	val-u test-u Rank
<i>Using Decimal Prediction Format</i>								
X_1, Y_1, X_2, Y_2	78.6	85.7	71.4	69.5	77.9	60.1	75.3	73.7 72.5 1.4
X_c, Y_c, W, H	78.5	85.4	70.6	68.8	78.2	58.7	75.4	72.8 71.8 2.4
X_1, Y_1, W, H	78.6	85.5	71.2	69.8	77.9	59.1	75.0	72.8 72.9 1.8
<i>Using Integer Prediction Format</i>								
X_1, Y_1, X_2, Y_2	79.4	86.0	72.1	70.9	79.4	60.5	76.3	73.9 73.3 1.4
X_c, Y_c, W, H	79.6	85.8	70.3	69.9	77.8	59.4	75.6	73.1 73.3 2.4
X_1, Y_1, W, H	79.7	85.7	72.2	70.3	79.0	60.3	75.4	72.2 73.5 2.0

Table 2. Performance comparison of different bounding box formats across benchmarks. The X_1, Y_1, X_2, Y_2 format consistently achieves the highest average rank in both *decimal* and *integer* formats, indicating its superiority over formats from traditional visual grounding methods and datasets in MLLMs.

hypothesis. We compute Spearman’s Rank Correlation between the similarity lists and the ground-truth ranking, respectively, and then average the results to obtain our final similarity-based correlation metric. A value closer to 1 supports the hypothesis, indicating that “closer coordinates exhibit higher token similarity.” Conversely, a value approaching -1 provides strong evidence against the hypothesis. Using the *integer* format, we obtain a correlation score of 0.6396 for the *one-hot* supervision format and 0.4680 for the *Gaussian label smoothing* format. This suggests that training with the *one-hot* format effectively encodes spatial semantics, with a stronger effect compared to the *Gaussian label smoothing* format.

3.4. Bounding Box Format

Now we discuss the choices on the format of bounding box based on *decimal* and *integer* prediction format.

- 1) X_1, Y_1, X_2, Y_2 . It is a widely-used bounding box format in autoregressive approach [4, 24, 49], where (X_1, Y_1) is the upper-left and (X_2, Y_2) is the lower-right coordinates.
- 2) X_c, Y_c, W, H . Some visual grounding methods, *e.g.* Deng et al. [6], Kang et al. [14], use center coordinates (X_c, Y_c) together with width and height (W, H) to indicate a bounding box. This format has not been adopted in previous MLLMs. Thus, we explore this design in MLLMs.
- 3) X_1, Y_1, W, H . It is the default bounding box format for benchmark datasets [16, 28], where (X_1, Y_1) is upper-left coordinates and (W, H) is width and height. This alternative has not been used in previous MLLMs and we explore this design in MLLMs.

Results. As shown in Tab. 2, the X_1, Y_1, X_2, Y_2 bounding box format consistently achieves the highest average rank in both *decimal* and *integer* formats. This demonstrates that the bounding box format used in existing visual grounding methods and the format used in datasets are less effective than the format used in autoregressive approaches.

4. Grounding Data Design

We explore the design choices for grounding data, including the synergistic effects of multitask training in Sec. 4.1, different ways to organize conversational data in Sec. 4.2, and the scaling property on training time in Sec. 4.3. Unless specified otherwise, we adopt the combination of the best performing choices as our grounding paradigm for the subsequent studies, specifically, the *normalized integer* in X_1, Y_1, X_2, Y_2 format with *one-hot* supervision.

4.1. Synergistic Effect

Multitask training is widely recognized as an effective approach to enhancing performance through its synergistic effects [24, 56]. However, it remains an open question whether multitask training is effective in attaining visual grounding ability within the same training budget. Here, we compare three settings.

1) *Visual grounding data*. The baseline is trained on our default data which consists of pure visual grounding data, as described in the Sec. 2.2.

2) *Visual grounding + VQA data*. To investigate the synergistic effect from multitask training, we incorporate the remaining VQA data from LLaVA-1.5’s 665K multimodal instruct tuning examples.

3) *Scaled visual grounding data*. To provide a fair comparison by using the same training budget, we scale the *visual grounding data* by randomly sampling and duplicating instances from the dataset until the total number of samples matches the *visual grounding + VQA data*.

Results. As shown in Tab. 3, *scaled visual grounding data* and *visual grounding + VQA data* demonstrate that, under the same training cost, using only visual grounding data is more effective than incorporating various VQA tasks in multitask training. Notably, *scaled visual grounding data* is constructed by simply duplicating samples from *visual grounding data* without introducing new unique samples. Therefore, given a fixed training budget, we believe that increasing the diversity in visual ground data is more effective than the synergistic effect from multitask training for building MLLM’s visual grounding ability.

4.2. Conversation Organization

In MLLMs [24, 25], each training data is structured as a multi-round conversation. Specifically, given an image, multiple image-related question-answering pairs are sequentially concatenated as one data sample. This structure influences the in-context learning in two key aspects, *duplicated annotations* and the *maximum number of conversation rounds*.

Duplicated Annotations. Given a fixed bounding box for an object, visual grounding data may include multiple referential sentences describing the object. Consequently, in

Format	RefCOCO			RefCOCO+			RefCOCOg		
	val	testA	testB	val	testA	testB	val-g	val-u	test-u
Visual grounding data	79.4	86.0	72.1	70.9	79.4	60.5	76.3	73.9	73.3
Visual grounding + VQA data	81.6	87.8	74.8	73.6	81.2	62.5	78.4	76.1	76.3
Scaled visual grounding data	85.2	90.3	79.3	76.8	84.3	67.8	85.4	78.2	78.7

Table 3. Comparison of different training data configurations to assess the synergistic effect. The results show that under the same training cost, using only visual grounding data (*scaled visual grounding data*) outperforms multitask training with both visual grounding and VQA data (*visual grounding + VQA data*).

Format	RefCOCO			RefCOCO+			RefCOCOg		
	val	testA	testB	val	testA	testB	val-g	val-u	test-u
<i>Using Decimal Prediction Format</i>									
Original	78.6	85.7	71.4	69.5	77.9	60.1	75.3	73.7	72.5
Deduplicate	83.3	88.8	76.9	75.1	82.7	66.8	80.1	77.3	77.0
Scaled Original	82.0	88.5	76.2	73.3	81.7	64.2	78.3	75.8	75.4
<i>Using Integer Prediction Format</i>									
Original	79.4	86.0	72.1	70.9	79.4	60.5	76.3	73.9	73.3
Deduplicate	83.9	89.2	77.4	75.1	83.3	66.6	80.6	77.6	77.5
Scaled Original	82.7	89.0	76.3	74.2	82.1	64.7	79.0	76.3	76.1

Table 4. Ablation study on the impact of duplicated annotations in conversational data. Results show that *deduplicated conversational data* consistently outperforms others across both *decimal* and *integer* prediction formats, emphasizing the importance of removing duplicated answer samples to enhance data quality.

conversational data, the answer (bounding box) for the current round’s question may have already appeared in a previous round, resulting in ground truth leakage and thereby weakens the training sample. To investigate this consideration, we perform the following ablation study:

1) *Original conversational data*. We use the original conversational data of visual grounding as described in Sec. 2.2 as the baseline.

2) *Deduplicated conversational data*. We extract question-answering pairs from the original data where answers are duplicated and create new conversational data from these pairs. This process is repeated iteratively until no datum contain duplicated answers, resulting in 161,827 samples.

3) *Scaled original data*. Since the *deduplicated conversational data* has 49,457 more data than the *original*, the training steps has been increased. To ensure a fair ablation study, we scale the *original* data by randomly repeating samples to match the number of samples in the *deduplicated* data.

Results. Tab. 4 lists the result of the ablation study on both *decimal* and *integer* prediction formats. The *deduplicated conversational data* consistently achieves superior performance, underscoring the importance of eliminating the duplicated answers, which prevents ground truth leakage and improves the quality of training data.

Maximum Round	RefCOCO			RefCOCO+			RefCOCOg			Ave.↓ Rank
	val	testA	testB	val	testA	testB	val-g	val-u	test-u	
One	85.8	90.8	80.0	77.8	84.9	68.9	81.7	78.7	79.1	8.7
Two (Scaled)	86.5	90.6	80.3	78.5	86.0	70.2	84.7	80.3	80.6	4.6
Three (Scaled)	86.7	91.0	80.8	79.5	85.9	71.0	85.7	79.7	80.7	2.9
Four (Scaled)	86.6	91.0	80.0	79.2	85.5	69.3	86.4	80.5	80.7	3.9
Five (Scaled)	86.6	90.9	79.5	79.6	86.0	69.7	86.6	80.4	80.4	3.8
Six (Scaled)	86.4	91.1	79.3	79.2	85.6	70.0	87.6	79.5	80.5	4.4
Seven (Scaled)	86.0	90.5	79.7	79.0	85.5	69.8	87.5	80.0	80.2	6.2
Eight (Scaled)	85.6	91.1	79.0	78.4	85.5	69.3	87.6	79.7	79.6	6.7
Nine (Scaled)	86.1	91.0	79.3	79.3	85.6	69.3	87.8	79.2	80.0	5.3
Ten (Scaled)	86.4	90.7	79.2	79.3	85.7	68.8	87.5	80.1	79.8	6.1

Table 5. Ablation study on the maximum number of conversation rounds. Setting the maximum number to three achieves the best balance, enhancing the model’s reasoning capability across different aspects of the image while preventing excessive ground truth leakage that could overly simplify training.

Epoch	RefCOCO			RefCOCO+			RefCOCOg			Ave.↓ Rank
	val	testA	testB	val	testA	testB	val-g	val-u	test-u	
One	84.7	89.8	78.5	76.2	84.0	67.9	81.1	78.1	78.4	7.0
Two	87.4	91.7	81.7	80.1	86.1	71.3	85.4	80.5	80.7	2.4
Three	87.4	91.6	81.1	80.1	86.2	71.3	87.5	81.3	81.4	2.1
Four	87.4	91.7	81.5	80.3	86.9	71.1	88.0	81.3	81.4	1.8
Five	87.0	91.1	80.2	80.0	86.1	71.2	89.0	81.1	80.3	4.0
Six	86.7	90.6	80.5	79.7	86.1	70.6	89.4	80.4	80.4	4.2
Seven	86.2	90.8	80.3	79.1	85.7	69.6	89.2	79.6	80.4	5.1

Table 6. Ablation study on the number of training epochs. The model achieves peak performance at four epochs, after which additional training yields negative returns.

Maximum Number of Conversation Rounds. Increasing the number of conversation rounds introduces greater challenges in comprehensively reasoning about different aspects of the image. However, it also inevitably reveals more identified objects in the answers (*i.e.*, ground truth bounding boxes), thereby reducing the difficulty of grounding in subsequent rounds of question-answering. Therefore, we conduct a comprehensive ablation study to determine the optimal maximum number of conversation rounds, ranging from one to ten. We use *deduplicated* data and split the conversational data into subsets by truncating conversations at the specified maximum round limit. For example, if the maximum round is set to 5, a 10-round conversation is split into two samples, each containing 5 rounds. To ensure a fair comparison, we scale each dataset by randomly repeating samples to the same amount of the one round data setting.

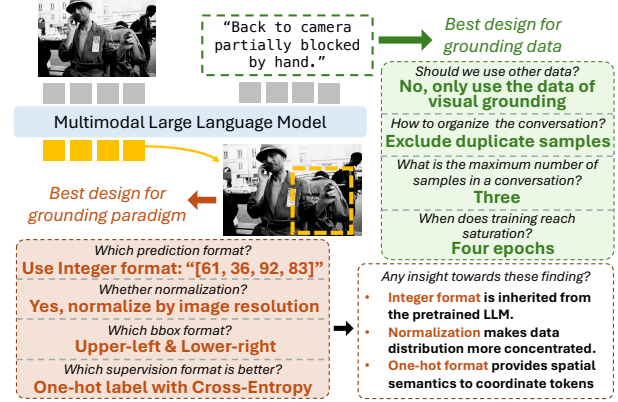


Figure 7. An overview of the best designs for training visual grounding in MLLM. We highlight key contributions, including optimal design choices on grounding paradigm and grounding data. We emphasize several insights towards our findings.

Results. As shown in Tab. 5, setting the *maximum number of conversations* to 3 achieves the best balance. This setting enhances the model’s ability to handle reasoning challenges across different aspects of the image while preventing excessive leakage of ground truth information, which could otherwise reduce training difficulty.

4.3. Scaling Training Time

To study the scaling property on training time when training visual grounding in MLLMs, we vary the training epochs from one to seven. Based on previous section, we use *deduplicated* data with *maximum three conversation rounds*.

Results. As shown in Tab. 6, training for 2 to 4 epochs results in strong performance, with 4 epochs yielding the best results. Performance improves significantly up to the second epoch, with marginal gains thereafter. Beyond the fourth epoch, additional training offers diminishing returns.

5. Summary & Conclusion

We present an empirical study on visual grounding in MLLMs based on LLaVA-1.5. Our study identifies optimal design choices and discusses the gained insights. As shown in Fig. 7, we propose to adopt the *normalized integer* format with the *upper-left and lower-right* bounding box representation, and train with *one-hot* labels using the cross-entropy loss. The *integer* format aligns with the pretrained LLM, while *normalization* mitigates long-tailed distributions. Our similarity-based correlation metric reveals that *one-hot* supervision enhances spatial semantics. For grounding data design, training on visual grounding data outperforms multitask training and removing duplicated answers improves learning. The optimal conversation round is three, and optimal training epoch is four. Integrating these designs, we significantly surpass LLaVA-1.5 by +5.6% / +6.9% / +7.0% on RefCOCO+/g. We believe our study lays a foundation for future research in advancing MLLM’s VG capability.

References

- [1] Peter Anderson, Xiaodong He, Chris Buehler, Damien Teney, Mark Johnson, Stephen Gould, and Lei Zhang. Bottom-up and top-down attention for image captioning and visual question answering. In *Proceedings of the IEEE conference on computer vision and pattern recognition*, pages 6077–6086, 2018. 1
- [2] Keqin Chen, Zhao Zhang, Weili Zeng, Richong Zhang, Feng Zhu, and Rui Zhao. Shikra: Unleashing multi-modal llm’s referential dialogue magic. *arXiv preprint arXiv:2306.15195*, 2023. 1, 2, 3, 4
- [3] Shizhe Chen, Qin Jin, Peng Wang, and Qi Wu. Say as you wish: Fine-grained control of image caption generation with abstract scene graphs. In *Proceedings of the IEEE/CVF conference on computer vision and pattern recognition*, pages 9962–9971, 2020. 1
- [4] Ting Chen, Saurabh Saxena, Lala Li, David J Fleet, and Geoffrey Hinton. Pix2seq: A language modeling framework for object detection. *arXiv preprint arXiv:2109.10852*, 2021. 1, 2, 3, 4, 6
- [5] Wei-Lin Chiang, Zhuohan Li, Zi Lin, Ying Sheng, Zhanghao Wu, Hao Zhang, Lianmin Zheng, Siyuan Zhuang, Yonghao Zhuang, Joseph E. Gonzalez, Ion Stoica, and Eric P. Xing. Vicuna: An open-source chatbot impressing gpt-4 with 90%* chatgpt quality, 2023. 1, 3, 4
- [6] Jiajun Deng, Zhengyuan Yang, Tianlang Chen, Wengang Zhou, and Houqiang Li. Transvg: End-to-end visual grounding with transformers. In *Proceedings of the IEEE/CVF International Conference on Computer Vision*, pages 1769–1779, 2021. 1, 3, 4, 6
- [7] Chuang Gan, Yandong Li, Haoxiang Li, Chen Sun, and Boqing Gong. Vqs: Linking segmentations to questions and answers for supervised attention in vqa and question-focused semantic segmentation. In *Proceedings of the IEEE international conference on computer vision*, pages 1811–1820, 2017. 1
- [8] Junwen He, Yifan Wang, Lijun Wang, Huchuan Lu, Jun-Yan He, Jin-Peng Lan, Bin Luo, and Xuansong Xie. Multi-modal instruction tuned llms with fine-grained visual perception. In *Proceedings of the IEEE/CVF Conference on Computer Vision and Pattern Recognition*, pages 13980–13990, 2024. 1, 2, 3, 4
- [9] Drew A Hudson and Christopher D Manning. Gqa: A new dataset for real-world visual reasoning and compositional question answering. In *Proceedings of the IEEE/CVF conference on computer vision and pattern recognition*, pages 6700–6709, 2019. 3
- [10] Weitai Kang, Mengxue Qu, Jyoti Kini, Yunchao Wei, Mubarak Shah, and Yan Yan. Intent3d: 3d object detection in rgb-d scans based on human intention. *arXiv preprint arXiv:2405.18295*, 2024. 1, 3
- [11] Weitai Kang, Mengxue Qu, Yunchao Wei, and Yan Yan. Actress: Active retraining for semi-supervised visual grounding. *arXiv preprint arXiv:2407.03251*, 2024. 1, 4
- [12] Weitai Kang, Luowei Zhou, Junyi Wu, Changchang Sun, and Yan Yan. Visual grounding with attention-driven constraint balancing. *arXiv preprint arXiv:2407.03243*, 2024. 1, 3, 4
- [13] Weitai Kang, Haifeng Huang, Yuzhang Shang, Mubarak Shah, and Yan Yan. Robin3d: Improving 3d large language model via robust instruction tuning, 2025. 1
- [14] Weitai Kang, Gaowen Liu, Mubarak Shah, and Yan Yan. Segvg: Transferring object bounding box to segmentation for visual grounding. In *European Conference on Computer Vision*, pages 57–75. Springer, 2025. 1, 3, 4, 6
- [15] Siddharth Karamcheti, Suraj Nair, Ashwin Balakrishna, Percy Liang, Thomas Kollar, and Dorsa Sadigh. Prismatic vlms: Investigating the design space of visually-conditioned language models. *arXiv preprint arXiv:2402.07865*, 2024. 1, 2, 3
- [16] Sahar Kazemzadeh, Vicente Ordonez, Mark Matten, and Tamara Berg. Referitgame: Referring to objects in photographs of natural scenes. In *Proceedings of the 2014 conference on empirical methods in natural language processing (EMNLP)*, pages 787–798, 2014. 1, 3, 6
- [17] Ranjay Krishna, Yuke Zhu, Oliver Groth, Justin Johnson, Kenji Hata, Joshua Kravitz, Stephanie Chen, Yannis Kalantidis, Li-Jia Li, David A Shamma, et al. Visual genome: Connecting language and vision using crowdsourced dense image annotations. *International journal of computer vision*, 123:32–73, 2017. 3
- [18] Xin Lai, Zhuotao Tian, Yukang Chen, Yanwei Li, Yuhui Yuan, Shu Liu, and Jiaya Jia. Lisa: Reasoning segmentation via large language model. In *Proceedings of the IEEE/CVF Conference on Computer Vision and Pattern Recognition*, pages 9579–9589, 2024. 3, 4
- [19] Hugo Laurençon, Léo Tronchon, Matthieu Cord, and Victor Sanh. What matters when building vision-language models? *arXiv preprint arXiv:2405.02246*, 2024. 1, 2, 3
- [20] Bin Lei, Yuchen Li, Yiming Zeng, Tao Ren, Yi Luo, Tianyu Shi, Zitian Gao, Zeyu Hu, Weitai Kang, and Qiuwu Chen. Infant agent: A tool-integrated, logic-driven agent with cost-effective api usage. *arXiv preprint arXiv:2411.01114*, 2024. 1
- [21] Liunian Harold Li, Pengchuan Zhang, Haotian Zhang, Jianwei Yang, Chunyuan Li, Yiwu Zhong, Lijuan Wang, Lu Yuan, Lei Zhang, Jenq-Neng Hwang, et al. Grounded language-image pre-training. In *Proceedings of the IEEE/CVF Conference on Computer Vision and Pattern Recognition*, pages 10965–10975, 2022. 1
- [22] Yanjie Li, Sen Yang, Peidong Liu, Shoukui Zhang, Yunxiao Wang, Zhicheng Wang, Wankou Yang, and Shu-Tao Xia. Simcc: A simple coordinate classification perspective for human pose estimation. In *European Conference on Computer Vision*, pages 89–106. Springer, 2022. 3, 5
- [23] Haotian Liu. Official codebase of llava-1.5. <https://github.com/haotian-liu/LLaVA>, 2023. 3
- [24] Haotian Liu, Chunyuan Li, Yuheng Li, and Yong Jae Lee. Improved baselines with visual instruction tuning. In *Proceedings of the IEEE/CVF Conference on Computer Vision and Pattern Recognition*, pages 26296–26306, 2024. 1, 2, 3, 4, 6, 7
- [25] Haotian Liu, Chunyuan Li, Qingyang Wu, and Yong Jae Lee. Visual instruction tuning. *Advances in neural information processing systems*, 36, 2024. 3, 7

- [26] Jiasen Lu, Christopher Clark, Rowan Zellers, Roozbeh Motlaghi, and Aniruddha Kembhavi. Unified-io: A unified model for vision, language, and multi-modal tasks. In *The Eleventh International Conference on Learning Representations*, 2022. 1
- [27] Jiasen Lu, Christopher Clark, Sangho Lee, Zichen Zhang, Savya Khosla, Ryan Marten, Derek Hoiem, and Aniruddha Kembhavi. Unified-io 2: Scaling autoregressive multimodal models with vision language audio and action. In *Proceedings of the IEEE/CVF Conference on Computer Vision and Pattern Recognition*, pages 26439–26455, 2024. 1
- [28] Junhua Mao, Jonathan Huang, Alexander Toshev, Oana Camburu, Alan L Yuille, and Kevin Murphy. Generation and comprehension of unambiguous object descriptions. In *Proceedings of the IEEE conference on computer vision and pattern recognition*, pages 11–20, 2016. 1, 3, 6
- [29] Maxime Oquab, Timothée Darcet, Théo Moutakanni, Huy Vo, Marc Szafraniec, Vasil Khalidov, Pierre Fernandez, Daniel Haziza, Francisco Massa, Alaaeldin El-Nouby, et al. Dinov2: Learning robust visual features without supervision. *arXiv preprint arXiv:2304.07193*, 2023. 1
- [30] Zhiliang Peng, Wenhui Wang, Li Dong, Yaru Hao, Shaohan Huang, Shuming Ma, and Furu Wei. Kosmos-2: Grounding multimodal large language models to the world. *arXiv preprint arXiv:2306.14824*, 2023. 1, 2, 3, 4
- [31] Bryan A Plummer, Liwei Wang, Chris M Cervantes, Juan C Caicedo, Julia Hockenmaier, and Svetlana Lazebnik. Flickr30k entities: Collecting region-to-phrase correspondences for richer image-to-sentence models. In *Proceedings of the IEEE international conference on computer vision*, pages 2641–2649, 2015. 1
- [32] Alec Radford, Jong Wook Kim, Chris Hallacy, Aditya Ramesh, Gabriel Goh, Sandhini Agarwal, Girish Sastry, Amanda Askell, Pamela Mishkin, Jack Clark, et al. Learning transferable visual models from natural language supervision. In *International conference on machine learning*, pages 8748–8763. PMLR, 2021. 1, 3
- [33] Hanoona Rasheed, Muhammad Maaz, Sahal Shaji, Abdelrahman Shaker, Salman Khan, Hisham Cholakkal, Rao M Anwer, Eric Xing, Ming-Hsuan Yang, and Fahad S Khan. Glamm: Pixel grounding large multimodal model. In *Proceedings of the IEEE/CVF Conference on Computer Vision and Pattern Recognition*, pages 13009–13018, 2024. 3
- [34] Zhongwei Ren, Zhicheng Huang, Yunchao Wei, Yao Zhao, Dongmei Fu, Jiashi Feng, and Xiaojie Jin. Pixellm: Pixel reasoning with large multimodal model. In *Proceedings of the IEEE/CVF Conference on Computer Vision and Pattern Recognition*, pages 26374–26383, 2024. 3, 4
- [35] Yuzhang Shang, Mu Cai, Bingxin Xu, Yong Jae Lee, and Yan Yan. Llava-prumerge: Adaptive token reduction for efficient large multimodal models. *arXiv preprint arXiv:2403.15388*, 2024. 1
- [36] ShareGPT. <https://sharegpt.com/>, 2023. 3
- [37] Min Shi, Fuxiao Liu, Shihao Wang, Shijia Liao, Subhashree Radhakrishnan, De-An Huang, Hongxu Yin, Karan Sapra, Yaser Yacoob, Humphrey Shi, et al. Eagle: Exploring the design space for multimodal llms with mixture of encoders. *arXiv preprint arXiv:2408.15998*, 2024. 1, 2, 3
- [38] Oleksii Sidorov, Ronghang Hu, Marcus Rohrbach, and Amanpreet Singh. Textcaps: a dataset for image captioning with reading comprehension. In *Computer Vision–ECCV 2020: 16th European Conference, Glasgow, UK, August 23–28, 2020, Proceedings, Part II 16*, pages 742–758. Springer, 2020. 3
- [39] Hugo Touvron, Thibaut Lavril, Gautier Izacard, Xavier Martinet, Marie-Anne Lachaux, Timothée Lacroix, Baptiste Rozière, Naman Goyal, Eric Hambro, Faisal Azhar, et al. Llama: Open and efficient foundation language models. *arXiv preprint arXiv:2302.13971*, 2023. 1
- [40] Hugo Touvron, Louis Martin, Kevin Stone, Peter Albert, Amjad Almahairi, Yasmine Babaei, Nikolay Bashlykov, Soumya Batra, Prajjwal Bhargava, Shriti Bhosale, et al. Llama 2: Open foundation and fine-tuned chat models. *arXiv preprint arXiv:2307.09288*, 2023. 1
- [41] Peng Wang, An Yang, Rui Men, Junyang Lin, Shuai Bai, Zhikang Li, Jianxin Ma, Chang Zhou, Jingren Zhou, and Hongxia Yang. Ofa: Unifying architectures, tasks, and modalities through a simple sequence-to-sequence learning framework. In *International conference on machine learning*, pages 23318–23340. PMLR, 2022. 1, 2, 4
- [42] Wenhui Wang, Zhe Chen, Xiaokang Chen, Jiannan Wu, Xizhou Zhu, Gang Zeng, Ping Luo, Tong Lu, Jie Zhou, Yu Qiao, et al. Visionllm: Large language model is also an open-ended decoder for vision-centric tasks. *Advances in Neural Information Processing Systems*, 36, 2024. 1
- [43] Xinyu Wang, Yuliang Liu, Chunhua Shen, Chun Chet Ng, Canjie Luo, Lianwen Jin, Chee Seng Chan, Anton van den Hengel, and Liangwei Wang. On the general value of evidence, and bilingual scene-text visual question answering. In *Proceedings of the IEEE/CVF Conference on Computer Vision and Pattern Recognition*, pages 10126–10135, 2020. 1
- [44] Bin Xiao, Haiping Wu, Weijian Xu, Xiyang Dai, Houdong Hu, Yumao Lu, Michael Zeng, Ce Liu, and Lu Yuan. Florence-2: Advancing a unified representation for a variety of vision tasks. In *Proceedings of the IEEE/CVF Conference on Computer Vision and Pattern Recognition*, pages 4818–4829, 2024. 1
- [45] Shiyu Xuan, Qingpei Guo, Ming Yang, and Shiliang Zhang. Pink: Unveiling the power of referential comprehension for multi-modal llms. In *Proceedings of the IEEE/CVF Conference on Computer Vision and Pattern Recognition*, pages 13838–13848, 2024. 1, 2, 3
- [46] Li Yang, Yan Xu, Chunfeng Yuan, Wei Liu, Bing Li, and Weiming Hu. Improving visual grounding with visual-linguistic verification and iterative reasoning. In *Proceedings of the IEEE/CVF Conference on Computer Vision and Pattern Recognition*, pages 9499–9508, 2022. 3
- [47] Zhengyuan Yang, Tianlang Chen, Liwei Wang, and Jiebo Luo. Improving one-stage visual grounding by recursive subquery construction. In *European Conference on Computer Vision*, pages 387–404. Springer, 2020. 1, 3
- [48] Zhengyuan Yang, Zhe Gan, Jianfeng Wang, Xiaowei Hu, Faisal Ahmed, Zicheng Liu, Yumao Lu, and Lijuan Wang. Unitab: Unifying text and box outputs for grounded vision-

- language modeling. In *European Conference on Computer Vision*, pages 521–539. Springer, 2022. [1](#)
- [49] Haoxuan You, Haotian Zhang, Zhe Gan, Xianzhi Du, Bowen Zhang, Zirui Wang, Liangliang Cao, Shih-Fu Chang, and Yinfei Yang. Ferret: Refer and ground anything anywhere at any granularity. *arXiv preprint arXiv:2310.07704*, 2023. [1](#), [2](#), [3](#), [4](#), [6](#)
- [50] Quanzeng You, Hailin Jin, Zhaowen Wang, Chen Fang, and Jiebo Luo. Image captioning with semantic attention. In *Proceedings of the IEEE conference on computer vision and pattern recognition*, pages 4651–4659, 2016. [1](#)
- [51] Licheng Yu, Patrick Poirson, Shan Yang, Alexander C Berg, and Tamara L Berg. Modeling context in referring expressions. In *Computer Vision—ECCV 2016: 14th European Conference, Amsterdam, The Netherlands, October 11–14, 2016, Proceedings, Part II 14*, pages 69–85. Springer, 2016. [1](#)
- [52] Licheng Yu, Zhe Lin, Xiaohui Shen, Jimei Yang, Xin Lu, Mohit Bansal, and Tamara L Berg. Mtnet: Modular attention network for referring expression comprehension. In *Proceedings of the IEEE Conference on Computer Vision and Pattern Recognition*, pages 1307–1315, 2018. [3](#)
- [53] Xiaohua Zhai, Basil Mustafa, Alexander Kolesnikov, and Lucas Beyer. Sigmoid loss for language image pre-training. In *Proceedings of the IEEE/CVF International Conference on Computer Vision*, pages 11975–11986, 2023. [1](#)
- [54] Haotian Zhang, Pengchuan Zhang, Xiaowei Hu, Yen-Chun Chen, Liunian Li, Xiyang Dai, Lijuan Wang, Lu Yuan, Jenq-Neng Hwang, and Jianfeng Gao. Glipv2: Unifying localization and vision-language understanding. *Advances in Neural Information Processing Systems*, 35:36067–36080, 2022. [1](#)
- [55] Haotian Zhang, Mingfei Gao, Zhe Gan, Philipp Dufter, Nina Wenzel, Forrest Huang, Dhruti Shah, Xianzhi Du, Bowen Zhang, Yanghao Li, et al. Mml. 5: Methods, analysis & insights from multimodal llm fine-tuning. *arXiv preprint arXiv:2409.20566*, 2024. [2](#), [3](#), [4](#)
- [56] Haotian Zhang, Haoxuan You, Philipp Dufter, Bowen Zhang, Chen Chen, Hong-You Chen, Tsu-Jui Fu, William Yang Wang, Shih-Fu Chang, Zhe Gan, et al. Ferret-v2: An improved baseline for referring and grounding with large language models. *arXiv preprint arXiv:2404.07973*, 2024. [1](#), [2](#), [3](#), [4](#), [7](#)

Investigating the Design Space of Visual Grounding in Multimodal Large Language Model

Supplementary Material

data	normalize	refcoco val	refcoco+ val	refcocog val-g
50%	Unnormalized	55.8	48.3	49.0
50%	Normalized	65.4	55.0	56.6
100%	Unnormalized	72.6	62.5	63.8
100%	Normalized	79.4	70.9	76.3
150%	Unnormalized	75.0	65.0	66.0
150%	Normalized	81.1	69.9	71.6

Table 7. The impact of data volume in our empirical studies.

Prediction	Normalization	refcoco val	refcoco+ val	refcocog val-g
Decimal	Unnormalized	60.2	49.7	48.9
Integer	Unnormalized	61.1	51.0	50.5
Integer	Normalized	65.2	54.9	55.2

Table 8. Generalization to other MLLM architecture about our empirical studies.

tions with $\{\text{decimal}, \text{integer}\}$ formats \times $\{\text{original}, \text{deduplicate}, \text{scaled original}\}$ organizations. In all cases, the best combinations consistently align with our findings: integer + one-hot + normalized + $[X1, Y1, X2, Y2]$ + deduplicate.

6. Impact of data volume

We analyze the impact by using 50%, 100%, and 150% of the data in Tab. 7. On the aspect of normalization type, the normalized type outperforms unnormalized type regardless of data volume – the conclusion is consistent with our finding in the main paper.

7. Generalization to other MLLM architecture and baseline selection

We provide experiments using Qwen2.5-VL architecture by training 1 epoch on our VG data in Tab. 8 to demonstrate the generalization of our findings to stronger MLLMs. The results show that on the prediction format and normalization type aspects, the *integer + normalized* type is better, which is consistent with our findings in the main paper.

8. Clarification on Cross-Factor

We have provided several important cross-factor studies in the main paper: (1) *Prediction format \times supervision strategy* We contain 8 combinations with $\{\text{decimal}, \text{integer}\}$ formats \times $\{\text{one-hot}, \text{equal}, \text{gaussian}, \text{gaussian.w}\}$ strategies. (2) *Prediction format \times normalization type* We contain 6 combinations with $\{\text{decimal}, \text{integer}, \text{decoder}\}$ formats \times $\{\text{normalized}, \text{unnormalized}\}$ types. (3) *Prediction format \times bbox format* We contain 6 combinations with $\{\text{decimal}, \text{integer}\}$ formats \times $\{[X1, Y1, X2, Y2], [Xc, Yc, W, H], [X1, Y1, W, H]\}$ formats. (4) *Prediction format \times conversation organization* We contain 6 combina-